Failsafe Innovative Electromechanical Actuator with Advanced Electric Motor Control Technique Against Single Point of Failure

Iñaki Iglesias Aguinaga
Electric Aircraft Lab
Fundación Tecnalia Research & Innovation
San Sebastián, Spain
inaki.iglesias@tecnalia.com

Giovanni Di Domenico
R&D Department
UMBRAGROUP Spa
Albanella, Italia
gdidomenico@umbragroup.com

Jorge Gorostiza Herrero
Electric Aircraft Lab
Fundación Tecnalia Research & Innovation
San Sebastián, Spain
jorge.gorostiza@tecnalia.com

Moreno D'Andrea
R&D Department
UMBRAGROUP Spa
Albanella, Italia
mdandrea@umbragroup.com

***Abstract*— Electromechanical actuators (EMAs) begin to have a greater presence in current aeronautic designs due to the energy efficiency and reliability advantages they can provide. However, the conventional mechanical design with a single combination of a ball screw and an electric motor is subject to scenarios in which a single point of failure can render it inoperative. This paper presents a failsafe innovative EMA that gives a solution to the most typical jamming issues of aeronautical electromechanical actuators, either due to ball screw or electric motor failures. Different electric motor synchronization techniques applicable to the presented mechanical EMA design are analysed, and the benefits of the most adequate control strategy, the virtual line-shafting (VLS), are validated. Finally, the implementation of the control algorithm in a simplified virtual test bench with promising results is shown. The obtained results demonstrate that the proposed novel EMA mechanical design can enhance the failsafe capabilities of the current EMA designs based on a single ball screw and motor combination.**

Keywords*— *aeronautics, electromechanical actuator, failsafe system, more electric aircraft, synchronization control technique, virtual line-shafting, electronic line-shafting

I. Introduction

Global warming and its most direct consequence, climate change, are making the governments legislate in favour of greenhouse gas emission cutting policies [1]. Transportation, responsible for around 66% crude oil consumption and 25% of carbon dioxide emissions and with increasing predictions of 80%, is one of the main targets of these laws [2]. Within transportation, the aviation industry is one of the most important agents in pollution.

In this scenario, more electric aircraft (MEA) trend has arisen as a solution to reduce emissions. This concept focuses on the usage of electrical power for driving the aircraft systems, typically powered by hydraulic, pneumatic, electrical, and mechanical energy [3]. This trend implies a significant development in aircraft power systems during the coming generation. Technologies such as distributed electrical networks, highly efficient electrical power converters, and EMAs will have to traverse through a development path to fit into the aeronautical standards.

The project leading to these results has received funding from the Clean Sky 2 Joint Undertaking under the European Union's Horizon 2020 research and innovation programme under Grant Agreement no. 755562.

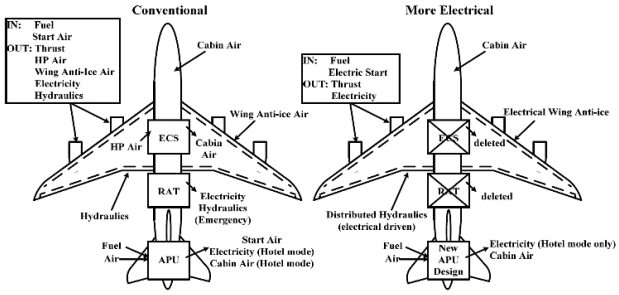

Fig. 1. Conventional (left) vs MEA (right) approach [4].

It is widely recognized that electrical actuation systems are a key enabling technology towards the MEA concept since they are in charge of driving flight control surfaces, landing gears, brakes, steering actuation, and other systems as doors, etc. [5]. However, the conventional mechanical topology used for this type of actuator based on a combination of an electric motor and a ball screw is subject to a mechanical single-point of failure.

This paper presents a novel concept of a failsafe electromechanical actuator to perform the extraction and retraction manoeuvre of the landing gear of a business jet, and the advanced control algorithm needed to drive this electromechanical actuator.

Section II is devoted to presenting the main architectural elements of the EMA and its operation modes. Then, Section III and IV go through different synchronization and low-level electric motor control algorithms. Finally, synchronization techniques are compared in Section V and conclusive remarks are shown in Section VI.

II. Failsafe EMA Description

The EMA mechanical design (Fig. 2) is described in this section. This fault-tolerant direct drive actuator is a patented system developed by UMBRAGROUP Spa (Patent number: EP3631243). This architecture is used for a generic landing gear (LG) application in a small aircraft. The invention uses two independent ball nuts, each one rigidly attached to its corresponding permanent magnet synchronous motor (PMSM) rotor and supported by two pairs of angular contact bearings. These ball nuts engage a common screw shaft, which has two different threaded portions on the outside diameter.

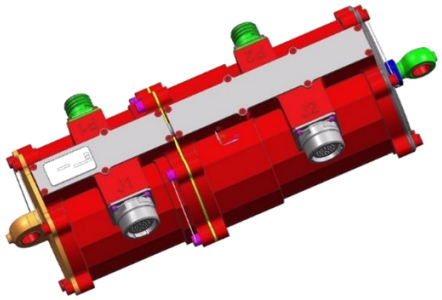

Fig. 2. Failsafe EMA 3D view.

This common screw shaft element has a double function, acting as a ball nut for the output shaft, and as a screw for the two external ball nuts. These three parts are kinematically connected, with the two independent ball nuts engaging the common screw shaft on the outside, and the output shaft engaging on the inside thread. Finally, the system is also equipped with two independent brakes, one for each ball nut.

This architecture comprises the following main components:

- The output shaft moves linearly and is connected to the landing gear.
- Three ball screw subsystems. The first one connects the ball nut 1 with the outer part of the common screw shaft, the second one connects ball nut 2 with the outer part of the common screw shaft, and the last one connects the output shaft with the inner part of the common screw shaft.
- Two electrical motors.
- Two electromechanical brakes.
- Two sets of bearings, one for each ball nut.

These components are schematically represented in Fig. 3.

A. Operation Modes

The proposed EMA system design has 4 different operating modes depending on the failure mode to avoid. As it can be observed in TABLE I, there are two modes (modes 3 and 4) where motor speed synchronization control is required to avoid the creation of force fighting conditions between motors that could lead to a system inefficiency or malfunction.

Mode 1 is defined as the nominal operating mode of the EMA, and a flow control flow diagram for the change between modes is proposed in Fig. 4, showing the change from one mode to another as the different failures are detected based on available sensors (speed sensors, stroke sensors and current sensors).

As it can be seen, due to the kinematical connection between all the mechanical parts of the EMA, the different operational modes 3 and 4 require a robust and precise speed synchronization technique to avoid force fighting.

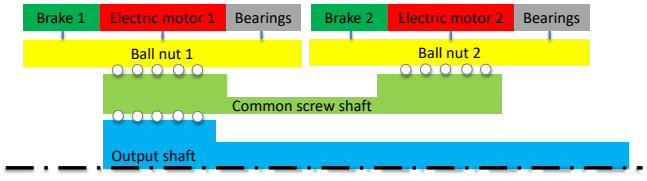

Fig. 3. Half section schematic representation of the main components of the failsafe EMA.

TABLE I. SUMMARY OF THE MAIN CHARACTERISTICS OF THE EMA WORKING MODES.

Mode	Operating mode	Failure avoidance/type	Motor synchronization
1 - Nominal	Motor 1 drives the EMA	Yes. Failure of Motor 2	Not required
2	Motor 2 drives the EMA	Yes. Failure of Motor 1	Not required
3	Both motors drive the EMA	Yes. Jamming of the output shaft with the screw shaft	Required
4	Both motors drive the EMA	Yes. Jamming of the screw shaft with one of the two ball nuts	Required

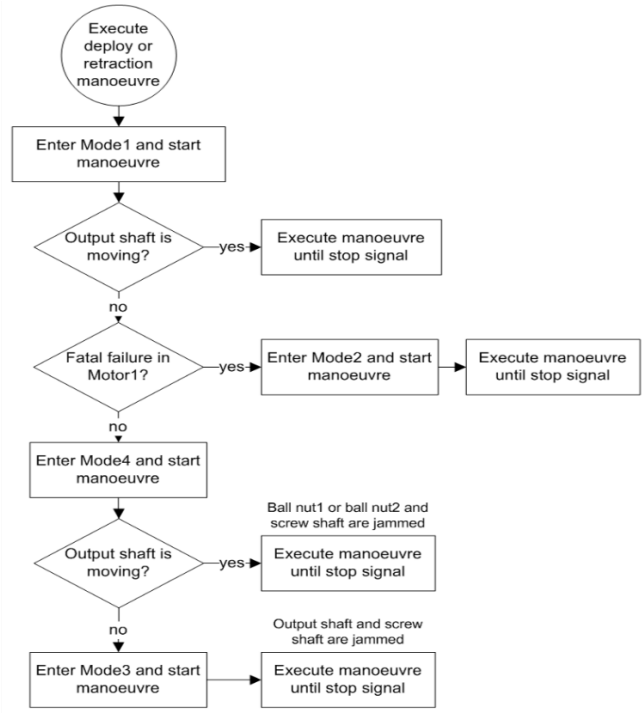

Fig. 4. Control flow diagram between the different modes depending on the detected failure.

III. SYNCHRONIZATION ALGORITHM

In the proposed innovative EMA concept, the two PMSMs are rigidly coupled by mechanical elements, and therefore the speed synchronization between them is a key parameter to make this concept work. An incorrect speed relation between the two electric motors would result in a force fighting scenario worsening the overall system energy efficiency. To overcome this problem, a synchronization control algorithm to regulate the speed of both motors is needed.

Although there are different techniques based on more advanced control techniques such as fuzzy, neural networks or sliding mode [7] only the most proven and robust techniques that have been extensively tested in the industrial application are evaluated, to guide the control towards a design that meets the aeronautical requirements of robustness and reliability.

A. Master-Slave Control

This corresponds to the simplest technique. In the master-slave control, both motors are arranged in a serial configuration (see Fig. 5). The angular speed setpoint ω_{SP} enters the controller of the master motor (motor #1) and its output angular speed ω_1 is then used as the reference to the slave motor (motor #2). Although this approach allows the slave motor to follow the motion of the master, it implies several practical drawbacks, such as a delay for the slave motor to reach the original reference speed [6]. T_{L1} and T_{L2} represent the load torque of each motor, and T_{SP1} and T_{SP2} represent the torque setpoint of each motor respectively.

Additionally, this topology presents a unidirectional synchronization. Even though this configuration enables the slave to react to the disturbances that alter the motion of the master, keeping the synchronization, disturbances in the slave are not reflected in the master behaviour [8]. As a result, during load impacts, synchronization between both motors cannot be ensured [9].

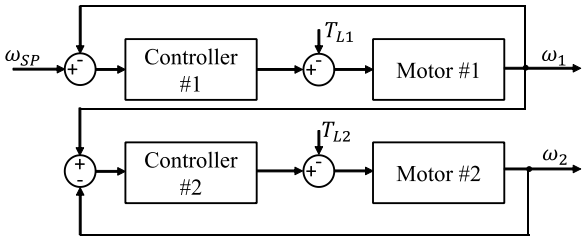

Fig. 5. Master-slave control algorithm scheme.

B. Cross-Coupling control

The cross-coupling control was first proposed by Koren to be applied to manufacturing systems [10]. This method was later further developed by Tomizuka, et al. [11] and Turl, et al. [12].

In this approach, the same angular speed setpoint ω_{SP} is used for both motors and each one tries to follow that input speed, according to the reduction ratios of each powertrain. The distinctive feature of this arrangement lies in the fact that the speed reference of each motor is modified according to an additional feedback signal proportional to the speed difference between both motors, $\omega_1 - \omega_2$ [7].

This topology uses this extra feedback signal as a relative speed monitoring signal, making any disturbance that affects the motion of one motor affect the speed reference of the other motors (see Fig. 6). When any motor suffers a disturbance and varies its output speed, the other motor detects the relative difference and adapts its speed to keep the synchronization [9].

This way, by selecting adequate tuning gains K_1 and K_2 for each motor, speed synchronization can be ensured.

The main drawback of this technique lies in tuning the gains, especially when working with more than two motors [6]. This is because small gains reduce the degree of synchronization, whereas increasing the gains amplifies the system noise and produces torque ripple. This handicap restricts the cross-coupling control to the synchronization of only two motors [8].

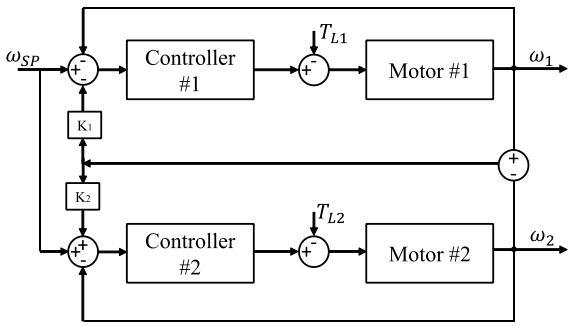

Fig. 6. Cross-coupling control algorithm scheme.

C. Virtual Line-Shafting Control

Considered the best approach for speed synchronization of motors, the virtual line-shafting control stems from a concept by Lorenz and Schmidt, who developed a motor synchronization method based on relative stiffness control [13]. Afterwards, this idea evolved into the virtual line-shafting method ([14], [15], [16], [17]) where this concept is applied to industrial applications where coordination was crucial, such as paper machines, winding machines, etc.

The virtual line-shafting approach is based on a model that emulates the mechanical line shaft that couples the motors. This is performed using a virtual shaft in charge of replicating the physical properties of the mechanical one (see Fig. 7).

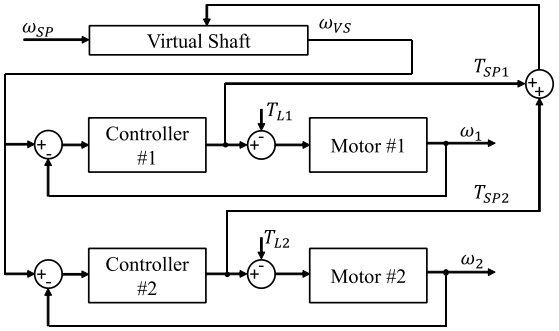

Fig. 7. Virtual line-shafting control algorithm scheme.

The output angular speed of this virtual shaft, ω_{VS}, acts as the angular speed setpoint for both motors, and thus each motor can be considered as a master motor [8]. Additionally, the torque setpoint of both motors, T_{SP1} and T_{SP2}, named in-shaft torques, are fed back as a disturbance to the virtual shaft [18]. When any disturbance distorts the motion of a motor, the virtual shaft detects it via the in-shaft torque and adjusts the output angular speed of the virtual shaft ω_{VS}, which allows for synchronization maintenance ([6], [19]).

This load-based approach makes the virtual line-shafting control show a good level of synchronization during the start-up and load-rejecting phases in steady-state conditions. However, since the relative position between motors cannot be guaranteed, it can be mainly used just for speed synchronization [9].

IV. Low-Level Motor Control – Field Oriented Control

Once the different synchronization strategies have been explained, it can be appreciated that all of them have in common the necessity of low-level speed control for each motor.

Field Oriented Control (FOC) and Direct Torque Control (DTC) ([20], [21]) are the two most popular vector control methods for electric motor drives. FOC uses linear controllers and pulse-width modulation (PWM) to control the fundamental components of the load voltage. On the other hand, DTC is a nonlinear strategy that directly generates the voltage vectors in the absence of a modulator.

Due to the sensitiveness to speed desynchronization of the failsafe innovative EMA presented in this paper and the high ripple derived from the DTC control [22], the FOC motor control algorithm is used for the low-level speed control [23].

V. Comparative Analisis Between motor Control Synchronization Algorithms

After analysing the different synchronization algorithms from the bibliography in the previous section, the master-slave synchronization technique does not provide the required performance to correctly synchronize both motors. For this reason, the following comparative study only covers the cross-coupling and the virtual line-shafting techniques, which are candidates for providing adequate accuracy and disturbance rejection performance.

This study is focused on analysing three main aspects that characterize the performance of each algorithm: the phase-currents, angular speed tracking, and more notably, the common screw shaft displacement difference due to the rotation of each motor independently due to the two different threaded portions. This feature is of special interest since it is responsible for the force fighting between the two electric motors driving the EMA.

To evaluate the response of each synchronization technique, the two motors are assumed to be rigidly coupled to a common screw shaft of negligible mass and inertia and all the currents measured serve to overcome the inertia of the motor itself and the counter-load created by the force-fighting between both motors. As it will be shown in section 5.2, this approximation seems reasonable as the common screw shaft displacement difference due to each motor rotation is low.

A purely kinematic model for the common screw shaft is being used and the output shaft kinematics have not been implemented as the main scope of the document is to compare the motor synchronization techniques.

A. Modelling and implementation

Both cross-coupling and virtual line-shafting synchronization strategies have been implemented in MATLAB/Simulink®. To implement each strategy, two identical blocks have been used, as it can be seen in Fig. 8 and Fig. 9. These blocks contain the following functionality:

- Controller model (one for each PMSM): it contains all the logic required by the FOC algorithm (angular speed controller, current controller, Clarke and Park direct and inverse transformations) to correctly generate the voltage setpoint vector.
- Power electronics model (one for each PMSM): it includes the logic required to simulate the PWM generation and the electronic circuit feeding the motor.
- PMSM model (two): it contains the modelling of the motor and EMA (electrical and dynamic). For simplicity, and as it is outside the scope of this paper, dynamic modelling of the PMSM has been reduced to the rotating motion of a mass.

Furthermore, in the virtual line-shafting synchronization strategy, a virtual shaft has been implemented with a simple PI controller. This virtual line-shaft is in charge of commanding the angular speed setpoint to each motor to reach synchronization.

The motors have a 10 to 1 speed ratio, which means that motor #1 will rotate 10 times faster than motor #2. Additionally, to implement the displacement difference and the two threaded portions of the screw shaft, a conversion using fixed pitch is used (p_1 and p_2), thus converting the angular speed of each motor (ω_1 and ω_2) into linear speed of the screw shaft due to the rotation of each motor (v_1 and v_2) ((1) and (2)).

Then, linear speed difference is computed and integrated over time to compute the displacement difference x_{disp} (3).

$$v_1 = \omega_1 \cdot p_1 \tag{1}$$

$$v_2 = \omega_2 \cdot p_2 \tag{2}$$

$$x_{disp} = \int_0^t (v_1 - v_2) \cdot \mathrm{d}t \tag{3}$$

It is important to mention that the parameters and gains of the PIDs for each model are identical for both control strategies, so that the comparison between both control strategies can be carried out.

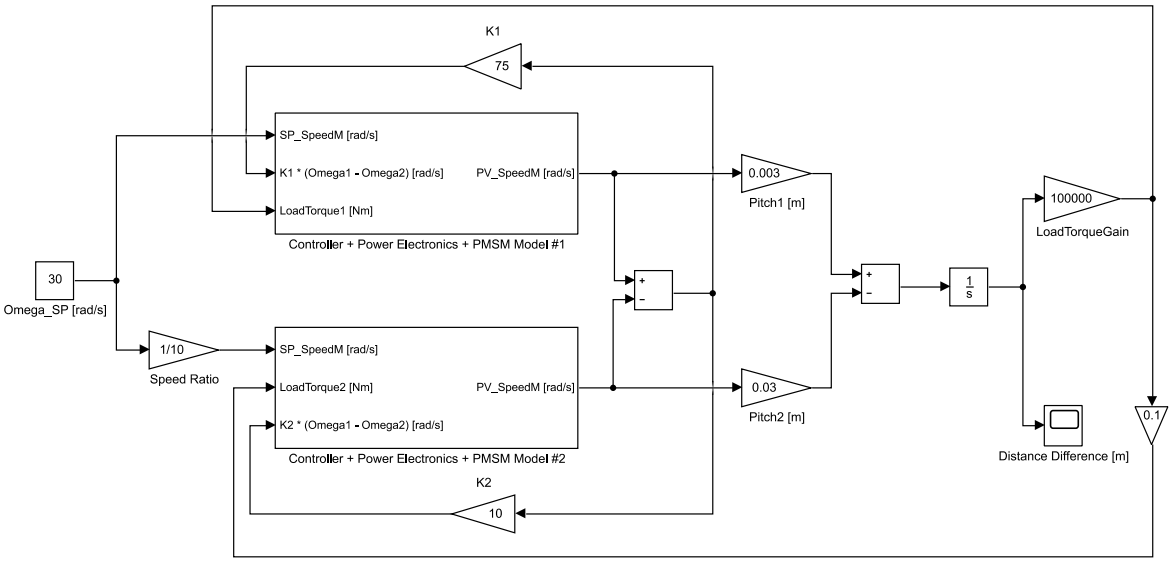

Fig. 8. Cross-coupling control strategy Simulink model.

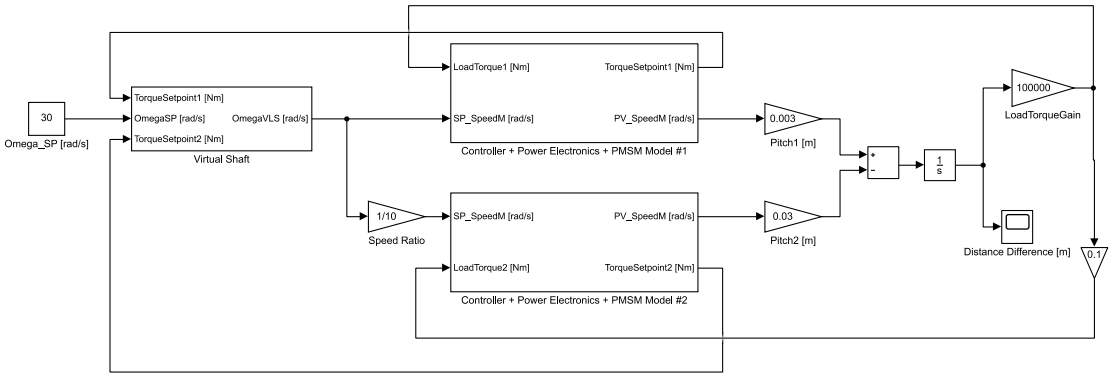

Fig. 9. Virtual Line-Shafting control strategy Simulink model.

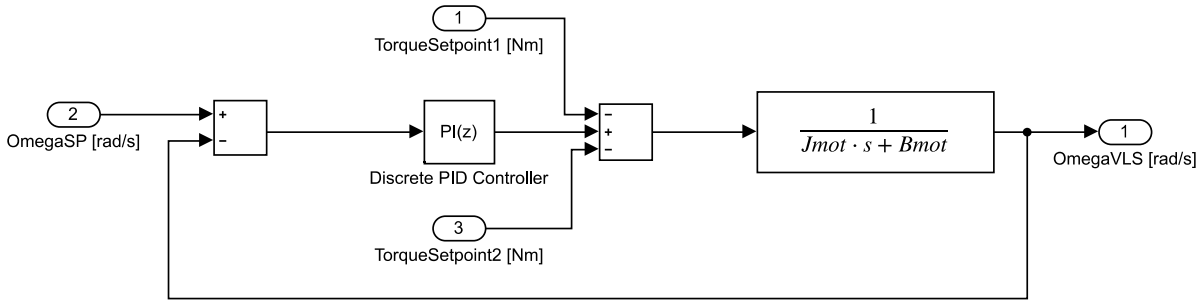

Fig. 10. Virtual shaft model.

B. *Simulink results*

To simulate both control strategies, an angular speed step setpoint ω_{SP} of 30 rad/s has been used.

The first relevant parameter in the simulations is the current consumption of each motor for both synchronization algorithms, which is a key indicator of the overall system efficiency.

In Fig. 11, Fig. 12, Fig. 13 and Fig. 14, the phase currents of each motor for both control strategies cross-coupling and virtual line-shafting are shown, evidencing that the cross-coupling strategy creates larger currents to operate the motors, and thus larger power consumption, whether the virtual line-shafting creates lower currents and therefore better EMA efficiency for the same output shaft displacement.

Fig. 15, Fig. 16, Fig. 17 and Fig. 18 show the speed tracking of each motor for each control strategy and is consistent with the current values presented in in Fig. 11, Fig. 12, Fig. 13 and Fig. 14, proving how the angular speed tracking of the virtual line-shafting strategy presents lower speed variations over the cross-coupling strategy.

The main difference between both synchronization techniques comes from the angular speed difference feedback corrections that are applied to the cross-coupling, which makes any motor angular speed difference turn into a disturbance that adds to the speed setpoint. This feedback disturbance is responsible for the motor speed oscillations, and therefore, for the higher current consumption.

Finally, the common screw shaft displacement difference is presented in Fig. 19 and Fig. 20 for both synchronization techniques, showing again that the virtual line shafting algorithm provides lower common screw shaft displacement difference values and thus lower force-fighting, which is an indicator of the EMA performance.

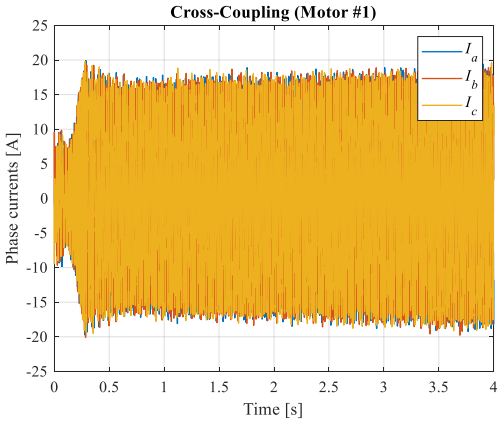

Fig. 11. Phase currents of motor #1 in cross-coupling.

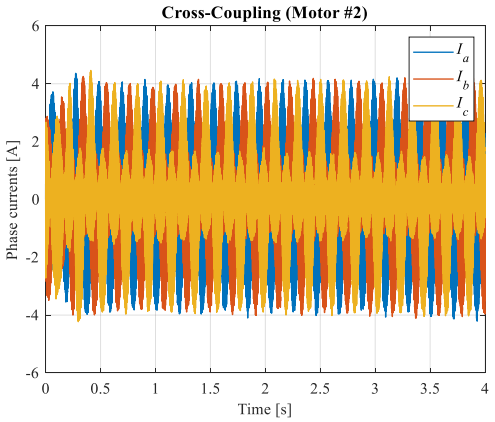

Fig. 12. Phase currents of motor #2 in cross-coupling.

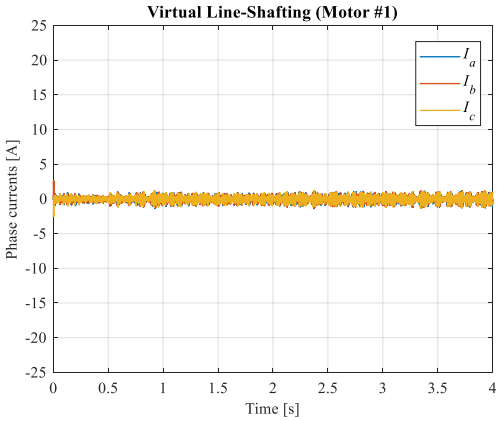

Fig. 13. Phase currents of motor #1 in VLS.

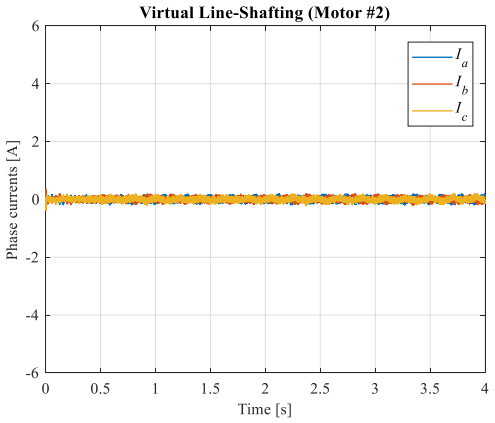

Fig. 14. Phase currents of motor #2 in VLS.

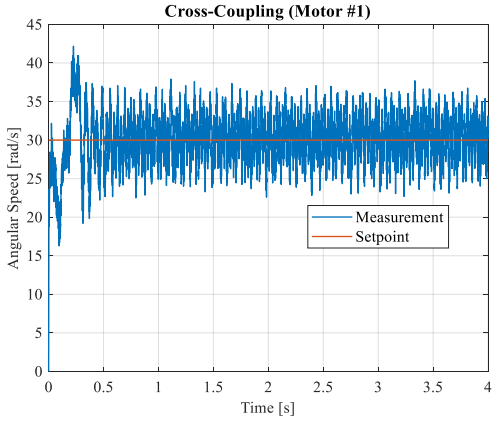

Fig. 15. Angular speed tracking of motor #1 in cross-coupling.

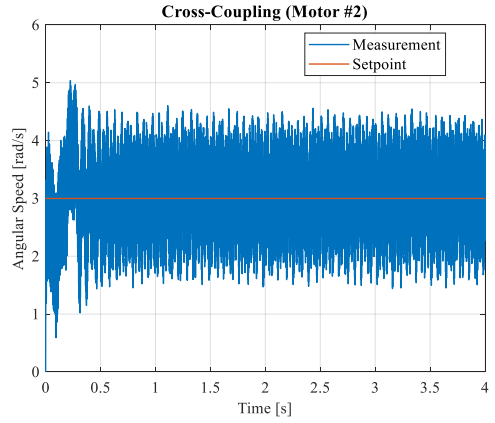

Fig. 16. Angular speed tracking of motor #2 in cross-coupling.

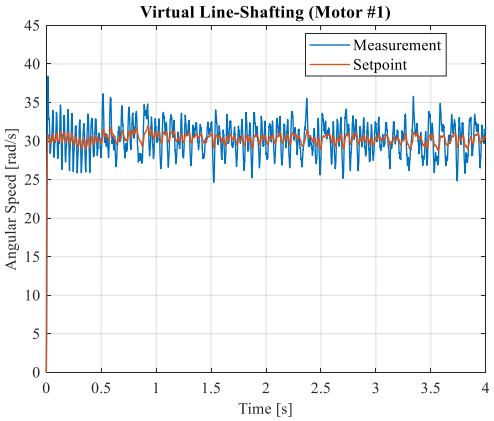

Fig. 17. Angular speed tracking of motor #1 in VLS.

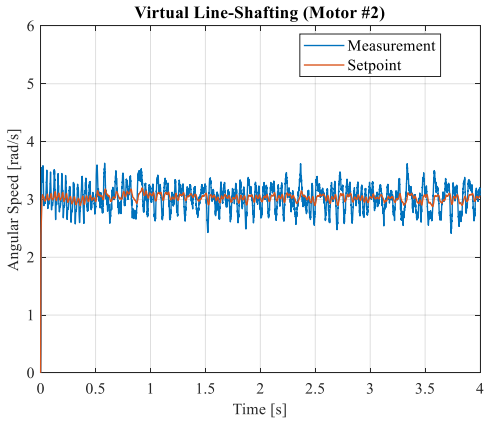

Fig. 18. Angular speed tracking of motor #2 in VLS.

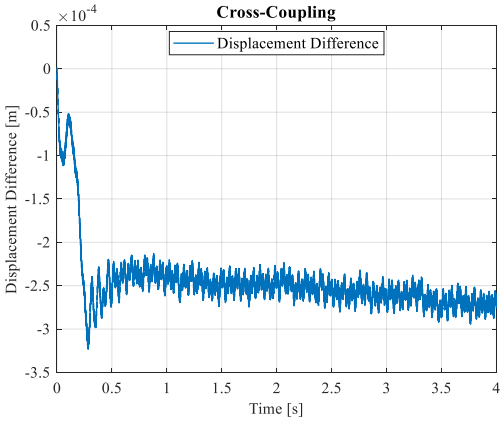

Fig. 19. Common screw shaft displacement difference for cross-coupling.

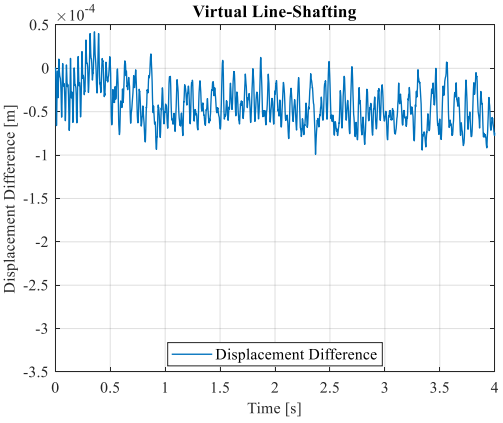

Fig. 20. Common screw shaft displacement for VLS.

VI. CONCLUSION

The mechanical design of the electromechanical actuator presented in this paper comprises a configuration with two electric motors and three ball screw subsystems, which provides additional capabilities to avoid the single point of failure problem.

After performing a literature-based preselection of the most promising synchronization strategies to avoid the force fighting between both electric motors of the electromechanical actuator, the simulation results have shown that the virtual line-shafting strategy is the best suited for the system in terms of accuracy and energy efficiency, showing the smaller displacement distance and lower current consumptions.

Additionally, this strategy also allows a smoother rotating speed variation, which could potentially decrease the mechanical jeopardy and increase the overall mechanical system's life expectancy.

The future work will include a more complex EMA modelling including different types of friction (e.g. bearings, ball screw), backlash between the different parts, and dynamic modelling of all the moving parts of the actuator as the objective of this paper was only to identify and select a suitable synchronization strategy for the system in terms of accuracy and current consumption.

REFERENCES

[1] European Comission, "2030 framework for climate and energy policies". http://ec.europa.eu/clima/policies/2030/index_en.htm

[2] S. Bozhko, C. I. Hill and T. Yang, "More-Electric Aircraft: Systems and Modeling", Wiley Encyclopedia of Electrical and Electronics Engineering, June 2018.

[3] X. Giraud, M. Budinger, X. Roboam, H. Piquet, M. Sartor and J. Faucher, "Optimal design of the Integrated Modular Power Electronics Cabinet", Aerospace Science and Technology, Vol 48, pp. 37-52, Oct. 2015.

[4] A.A. AbdElhafez and A.J. Forsyth, "A review of More Electric Aircraft", 13th International Conference on Aerospace Sciences & Aviation Technology (ASAT-13), Cairo, Egypt, May 26-28, 2009

[5] J. Li, Z. Yu, Y. Huang and Z. Li, "A review of electromechanical actuation systems for more electric aircraft", 2016 IEEE/CSAA International Conference on Aircraft Utility Systems (AUS), Beijing, China, Oct. 10-12, 2016.

[6] J. Li, Y. Fang, X. Huang and J. Li, "Comparison of Synchronization Control Techniques for Traction Motors of High-Speed Trains", Proceedings of the 17th International Conference on Electrical Machines and Systems (ICEMS), Hangzhou, China, Oct. 22-25, 2014.

[7] H. Huang, Q. Tu, C. Jiang, L. Ma, P. Li and H. Zhang, "Dual motor drive vehicle speed synchronization and coordination control strategy", AIP Conference Proceedings, Vol 1955, No 1, pp. 1-9, Dec. 9-13, 2018.

[8] J. Lemmens and J. Driesen, "Synchronization and efficiency analysis of a direct-drive multi-motor application", Proceedings of the 6th IET International Conference on Power Electronics, Machines and Drives (PEMD 2012), Bristol, UK, Mar. 27-29, 2012.

[9] F.J. Pérez-Pinal, C. Núñez, R. Álvarez and I. Cervantes, "Comparison of Multi-motor Synchronization Techniques", Proceedings of the 30th Annual Conference of the IEEE Industrial Electronics Society, Busan, Korea, Nov. 2-6, 2004.

[10] Y. Koren, "Cross-Coupled Biaxial Computer Control for Manufacturing Systems", Journal of Dynamic Systems, Measurement and Control, Vol 102, pp. 265-272, Dec. 1980.

[11] M. Tomizuka, J. Hu, G. Chiu and T. Kamano, "Synchronization of Two Motion Control Axes Under Adaptive Feedforward Control", Journal of Dynamic Systems, Measurement and Control, Vol 114, No. 2, pp. 196-203, Jun. 1992.

[12] G. Turl, M. Sumner and G.M. Asher, "A synchronized multi-motor control system using sensorless induction motor drives", Proceedings of the 2002 International Conference on Power Electronics, Machines and Drives, Santa Fe, NM, USA, Jun 4-7, 2002.

[13] R.D. Lorenz and P. Schmidt, "Synchronized motion control for process automation", Conference Record of the IEEE Industry Applications Society Annual Meeting, San Diego, CA, USA, Oct. 1-5, 1989.

[14] K. Payette, "The virtual shaft control algorithm for synchronized motion control", Proceedings of the 1998 American Control Conference (ACC), Philadelphia, PA, USA, Jun. 26, 1998.

[15] A. Valenzuela and R.D. Lorenz, "Electronic line-shafting control for paper machine drives", IEEE Transactions on Industry Applications, Vol 37, No 1, pp. 158-164, Feb. 2001.

[16] J. He, X. Chen, S.Mao, C. Zhang and J. Liu, "Virtual Line Shafting-Based Total-Amount Coordinated Control of Multi-Motor Traction Power", Wiley-Hindawi, Journal of Advanced Transportation, Volume 2020, Article ID 4735397, 9 pages, 2020.

[17] Z. Ting, L. Hong, F. Wei, L. He, L. Qi, X. Yifan, "Research on Dual Drive Synchronization Performance Based on Virtual Shaft Control Strategy", 2nd International Conference on Robotics and Automation Engineering, 2015.

[18] Q. geng, W. Liu, H. Wang, Z. Zhou and G. Zhang, "An Improved Electronic Line Shafting Control for Multimotor Drive System Based on Sliding Mode Observer", Hindawi, Mathematical Problems in Engineering, Volume 2019, Article ID 7064141, 13 pages, 2019.

[19] C. Zhang, Y. Xiao, J. He, and M. Yan, "Improvement of electronic line-shafting control in multi-axis systems," International Journal of Automation and Computing, vol. 15, no. 4, pp. 474–481, 2016.

[20] I. Takahashi and T. Noguch, "A new Quick-Response and High-Efficiency Control Strategy of an Induction Motor", IEEE Transactions on Industry Applications, Vol IA-22, No 5, pp. 820-827, Sep. 1986.

[21] U. Baader, M. Depenbrock and G. Gierse, "Direct self-control (DSC) of inverter-fed induction machine: a basis for speed control without speed measurements", IEEE Transactions on Industry Applications, Vol 28, No 3, May 1992.

[22] M.F. Rahman, M.E. Haque, L. Tang and L. Zhong, "Problems Associated with the Direct Torque Control of an Interior Permanent-Magnet Synchronous Motor Drive and Their Remedies", IEEE Transactions on Industrial Electronics, Vol 51, No 4, pp. 799-809, Aug. 2004.

[23] F. Wang, Z. Zhang, X. Mei, J. Rodríguez and R. Kennel, "Advanced Control Strategies of Induction Machine: Field Oriented Control, Direct Torque Control and Model Predictive Control", Energies, Vol 11, No 120, Jan. 2018.